Solubilities of carbon dioxide and water in rhyolitic melt at 850°C and 750 bars

Article *in* Earth and Planetary Science Letters · September 1993

DOI: 10.1016/0012-821X(93)90004-S

3 authors, including:

Jen Blank
NASA
59 PUBLICATIONS **3,734** CITATIONS
SEE PROFILE

Michael R. Carroll
University of Camerino
121 PUBLICATIONS **7,011** CITATIONS
SEE PROFILE

Earth and Planetary Science Letters, 119 (1993) 27–36
Elsevier Science Publishers B.V., Amsterdam

[CL]

Solubilities of carbon dioxide and water in rhyolitic melt at 850°C and 750 bars

J.G. Blank [a], E.M. Stolper [a] and M.R. Carroll [b]

[a] *California Institute of Technology, Division of Geological and Planetary Sciences, 170-25, Pasadena, CA 91125, USA*
[b] *University of Bristol, Department of Geology, Wills Memorial Building, Queens Road, Bristol BS8 1RJ, UK*

Received October 26, 1992; revision accepted June 11, 1993

ABSTRACT

Concentrations of carbon dioxide and water dissolved in glasses quenched from rhyolitic melts equilibrated with H_2O–CO_2 fluids at 850°C and 750 bar were measured using infrared spectroscopy; concentrations of H_2O and CO_2 in the quenched fluids were measured manometrically. The mole fraction of CO_2 in the quenched fluid ranged from 0.06 to 0.91. Concentrations of CO_2 in the coexisting rhyolitic melt increased from 23($\pm$6) ppm for the sample equilibrated with the most CO_2-poor fluid to 515($\pm$16) ppm for that equilibrated with the most CO_2-rich fluid. The water content of the melt varied from 0.51($\pm$0.06) to 3.34($\pm$0.08) wt%.

Our results show that concentrations of molecular CO_2 and H_2O in the glasses obey Henry's Law; i.e., the mole fractions of molecular CO_2 and molecular H_2O in the quenched melts are proportional to their fugacities in the coexisting vapor. CO_2 contents of vapor-saturated melts are not enhanced by addition of water to CO_2-rich vapor, contrary to previous reports for silicate melts at higher pressures. The Henrian behavior of CO_2 and H_2O at low pressure considerably simplifies modeling of the degassing of silicic magmas.

1. Introduction

Water and carbon dioxide are the most abundant volatile components in terrestrial magmas [1–5]. They exsolve from molten silicate into bubbles as magmas rise toward the earth's surface and depressurize. The vapor exsolving from magmas can be almost pure CO_2 at high pressure but becomes progressively enriched in H_2O upon decompression because carbon dioxide is much less soluble than water in most silicate liquids [e.g., 6,7]. On eruption at the surface all but a few ppm CO_2 and 0.1–0.2 wt% H_2O have typically partitioned into bubbles or escaped into the atmosphere [8–10]. Escape of these and other gases from magmas in near-surface environments is a significant factor in powering explosive volcanic eruptions [11,12] and is the ultimate source of the earth's atmosphere and oceans [13].

Key to understanding degassing phenomena of magmas are the solubilities of carbon dioxide and water in silicate liquids similar in composition to magmas, and there has been much work over many decades directed toward this goal [14–23]. It is frequently assumed in efforts to model the volatile contents of magmas that Henry's Law is obeyed for gaseous species dissolved in silicate melts [10,24–28]; i.e., the fugacity (or partial pressure at sufficiently low total pressure) of a gaseous species is assumed to be proportional to the amount dissolved in the melt. If valid, this assumption considerably simplifies modeling of degassing of systems with both water and carbon dioxide since it means that one need only determine the behavior of the end-member systems (i.e., silicate–CO_2 and silicate–H_2O) and the equation of state of mixed H_2O–CO_2 vapor. A potential complication, however, is that water may influence the solubility of carbon dioxide in silicate melts and vice versa. Thus it is essential that experimentation on the partitioning of water and carbon dioxide between vapor and silicate

melt in systems containing *both* volatile components be conducted. Indeed, although most efforts to model degassing phenomena have assumed Henrian behavior, studies conducted to date on mixed-volatile systems have reported significant deviations from Henry's Law [7,19,29–33]. Specifically, the addition of water to carbon-dioxide bearing systems has been reported to *increase* the amount of carbon dioxide that dissolves in vapor-saturated silicate melt, even though this leads to a *decrease* in the fugacity of CO_2 in the coexisting fluid. This result is important both because it has relevance for understanding degassing of magmas and because it has been viewed as providing insights into molecular-scale mechanisms by which water and carbon dioxide are incorporated into silicate liquids.

In this paper, we report results of an experimental study of the amounts of water and carbon dioxide that dissolve in rhyolitic liquid coexisting with vapor containing known amounts of both of these volatile components at 850°C and a total pressure of 750 bar. The results are used to evaluate the validity of Henry's Law in the low pressure range relevant to magma degassing. They are directly applicable to natural volcanic systems since recent work has suggested that vapor rich in both water and carbon dioxide plays a role in the evolution of high-level silicic magmatic systems [10,25,27].

2. Experimental and analytical methods

Rhyolitic obsidian from the Glass Buttes extrusive dome in Oregon was used as starting material; its composition is given in Dobson et al. [34]. Silver oxalate ($Ag_2C_2O_4$) powder, liquid (doubly distilled, and deionized) water and rhyolitic glass chips (sieved to 500–1000 μm in size) were loaded in known proportions into Pt capsules (28 mm $L \times 3.8$ mm $d \times 0.2$ mm wall thickness) that were then welded shut and pressurized with water in rapid-quench cold seal pressure vessels (René 41 alloy). The experiments were conducted at 850°C and 750 bar for approximately 6 days. The samples were magnetically levitated inside a vertical pressure vessel; at the end of an experiment, the magnet was removed and the sample dropped to a water-cooled portion of the pressure vessel where it cooled nearly isobarically (pressure increased by 25–30 bar during the quench) to room temperature in 2–3 s [35].

After quenching, sealed capsules were dried, weighed, and then placed on a vacuum line. The capsules were pierced, and their vapor was slowly transferred to a liquid nitrogen trap. Several hours were necessary for complete transfer of the water vapor, during which time the capsule was periodically heated with a hot air gun. Afterwards, < 1 μmole of non-condensable gas were pumped away. Carbon dioxide was distilled from water cryogenically with a -115°C slurry of 'M17' (furfural: $C_5H_4O_2$) and dry ice; the water ice that remained was evaporated and then converted to H_2 by being passed over hot uranium at 800°C [36]. Hydrogen and carbon dioxide were transferred separately into a manometer with a Toepler pump and their quantities measured. Blanks for H_2 and CO_2 were measured by pumping from the main portion of the line to the manometer with the Toepler pump for 0.5 h for each gas and were ~ 0.5 μmole and ~ 0.3 μmole. Yields of H_2 and CO_2 from the experimental charges were corrected for these blanks.

Concentrations of carbon dioxide and water dissolved in the quenched glasses were determined from transmission infrared spectra of doubly polished glass plates. One fragment from each experimental charge was analyzed. The analytical methods are similar to those described for water in Newman et al. [9] and for CO_2 by Blank et al. [37–39]. Samples were placed in the microchamber of a Nicolet 60SX FTIR spectrometer, and spectra were taken with 1024 scans, a gain of 32, a KBr beamsplitter, a visible light source, and a liquid-N_2 cooled, InSb detector. Round apertures (37 μm in diameter) in metal foils were used as masks to aim the infrared beam at selected regions of the polished glass fragment. Spectra were taken at 3–5 spots on each polished piece, including regions near the centers and edges of each glass fragment analyzed.

Water is dissolved in the quenched glasses both as hydroxyl groups (OH^-) and molecules of water (H_2O_{mol}), the concentrations of which were determined by Beer's Law from the intensities of absorptions at 4500 cm^{-1} (OH^-) and 5200 cm^{-1} (H_2O_{mol}) using molar absorptivities from Newman et al. [9], glass densities calculated iteratively

using their dependence on water content in glasses quenched from similar conditions [23], and the measured sample thicknesses. For most samples, the reported total dissolved water content is the sum of the amounts of water dissolved in these two forms. Glass from Experiment 9 had a low bulk water content (0.51 ± 0.06 wt%) and contained an amount of dissolved molecular water below the detection limit (≈ 0.05 wt%); the total dissolved water for this sample was determined from the intensity of the absorption at 3550 cm^{-1} using the molar absorptivity from Dobson et al. [34]. Concentrations of dissolved carbon dioxide molecules were determined using the intensity of the absorption at 2350 cm^{-1} [40] and the molar absorptivity from Blank [38]. Each sample spectrum was also checked in the 1300–1800 cm^{-1} region using a Globar light source, a CaF_2 beamsplitter, and a HgCdTe (MCT) detector for absorbances at 1365 cm^{-1} and 1610 cm^{-1} due to carbonate ions. These bands have been observed in a CO_2-rich (≈ 0.43 wt% total dissolved CO_2) rhyolitic glass quenched from 1550°C and 25 kbar [40], but they were absent in our samples. Baselines for all spectra were fit by smooth curves.

3. Results and discussion

The run conditions and analytical results are reported in Table 1.

All samples quenched to glass. Concentrations of dissolved CO_2 molecules in the glasses increased from $23(\pm 6)$ ppm for a sample equilibrated with the most CO_2-poor vapor to $515(\pm 16)$ ppm for that equilibrated with the most CO_2-rich vapor. The amount of total dissolved water in the glass varied from $0.51(\pm 0.06)$ to $3.34(\pm 0.08)$ wt% over the range of vapor compositions. The samples were homogeneous (within error) with respect to dissolved volatile contents. Microlites were present in the starting material and in several of the run products but were absent in the quenched run products with the highest dissolved water contents (Table 1). Bubbles were enclosed in the glass in several of the samples (Table 1); constituting less than ≈ 2 vol% of the enclosing glass, these bubbles ranged in diameter from approximately 5 to 30 μm but were usually smaller than 10 μm in diameter.

The mole fraction of CO_2 in the final vapor, $X^v_{CO_2}$, varied from 0.06 to 0.91. Amounts of water and carbon dioxide in the vapor as measured manometrically and calculated assuming mass balance (i.e., H_2O and CO_2 contents of the vapor calculated as the difference between the total H_2O and CO_2 loaded into the capsule, including the small amount initially present in the glass, and the amounts in the glass at the close of the experiment based on the infrared measurements) are in excellent agreement, as shown by the close correspondence of the results shown in Fig. 1 to the 1:1 line. The CO_2 mass balance is effectively independent of the CO_2 content of the quenched glass because < 1 μmole is dissolved in the glass compared to tens to hundreds of micromoles in the vapor. This is not the case for water which has much higher solubility in the melt. There is a small deficiency in the manometric measurements of the water contents of the vapor compared to the mass balance estimates. The reason for this is uncertain, but it may reflect incomplete removal of H_2O vapor from the platinum sample capsule (e.g., either because CO_2 is more readily removed during vacuum extraction or because of the unaccounted for contribution of bubbles trapped in the quenched glasses). The important point is that the values for $X^v_{CO_2}$ determined using the two different methods agree very well, in no case differing by more than 0.02 (Table 1).

In the data analysis below we used $X^v_{CO_2}$ determined from the manometric measurements of vapor composition as a basis for calculating CO_2 and H_2O fugacities (except for Experiment 3, for which the mass-balance calculated value had to be used because the CO_2 vapor collected from the capsule was lost). Doing so allowed us to avoid uncertainties due to propagation of errors in the amounts of liquid water and silver oxalate powder loaded into an experimental charge and in the measured concentrations of volatiles dissolved in the quenched glasses.

Our treatment assumes that the vapor in the capsule consisted entirely of CO_2 and H_2O, but other C-O-H gases must also be present. If, as is usually supposed to be the case [41], the f_{H_2} inside the capsule is identical to that in the water outside the capsule in equilibrium with the Ni-rich René bomb (at an f_{O_2} approximately one order of magnitude above Ni-NiO [42]), then we would

TABLE 1

Summary of results of experiments conducted at 850°C and 750 bar for ≈ 6 days

Experiment No.	2	3	4	5	7	9	10
vapor							
H_2O (liq.) loaded into capsule (μmol)	389	389	596	389	200	120	176
CO_2 (as $Ag_2C_2O_4$) loaded (μmol)	604	395	28	42	52	438	228
H_2O vapor (μmol) (mass balance)[a]	284(19)	273(20)	403(19)	218(21)	84(20)	49(17)	92(20)
H_2O vapor (μmol) (manometry)[b]	280	258	395	193	86	43	86
CO_2 vapor (μmol) (mass balance)[a]	604	395	28	42	51	437	228
CO_2 vapor (μmol) (manometry)[b]	601	*	26	43	50	427	224
dissolved volatiles							
Weight of rhyolitic glass chips (g)	0.10026	0.10013	0.0999	0.10029	0.10019	0.09967	0.0999
Amt. of water in initial glass (μmol)[c]	8.9 (2.8)	8.9 (2.8)	8.9 (2.8)	8.9 (2.8)	8.9 (2.8)	8.9 (2.8)	8.9 (2.8)
Dissolved total water (wt%)[d]	1.88 (.06)	2.24 (.08)	3.34 (.08)	3.23 (.10)	2.28 (.08)	0.51(.06)	1.35 (.10)
" " " (μmol)	105(5)	125(6)	185(6)	180(7)	127(6)	28(3)	75(6)
Dissolved OH (wt%)[e]	1.2(.04)	1.31(.06)	1.43(.06)	1.38(.06)	1.53(.06)	0.47(.04)	0.97(.04)
Dissolved mol H_2O (wt%)[e]	0.68(.02)	0.93(.03)	1.91(.06)	1.85(.04)	0.75(.04)	0.04(.10)	0.38(.08)
Calc. dissolved molecular H_2O (wt%)[f]	0.48	0.66	1.26	1.14	0.68	0.05	0.28
Dissolved CO_2 (ppm)[g]	389 (17)	260 (10)	23 (6)	80 (6)	196 (10)	515 (16)	406 (10)
" " (μmol)	0.9(.04)	0.6(.02)	<0.1(.01)	0.2(.02)	0.4(.02)	1.2(.04)	0.9(.02)
Remarks[h]	m	c,b	c	c	c,b	m,c	m,b
No. of IR analyses	4	4	5	4	3	3	3
mole fractions and fugacities [i,j]							
$X^{v}_{CO_2}$ (mass balance)	0.68(.01)	0.52(.01)	0.06(.01)	0.16(.01)	0.38(.02)	0.9(.01)	0.71(.01)
$X^{v}_{CO_2}$ (manometry)	0.68		0.06	0.18	0.37	0.91	0.72
f_{H2O} (bars)	197	305	631	547	411	53	171
f_{CO2} (bars)	604	452	45	143	312	820	642
$10^4 X^{m}_{CO_2}$	2.80	1.87	0.17	0.57	1.41	3.72	2.92
$100 X_B$	3.04	3.77	5.87	5.48	4.04	0.92	2.41
$100 X_{H2O,mol}$ (calculated)	0.79	1.15	2.20	2.04	1.24	0.11	0.52

* Vapor lost

[a] Amount of H_2O in the final vapor is calculated as {amount of initial water vapor + amount of initial dissolved water-amount of final dissolved water}. Amount of CO_2 in the final vapor is calculated as {amount of initial CO_2 vapor-amount of dissolved CO_2}. Numbers in parentheses are uncertainties in the water content of the vapor based on propagation of errors in initial and final water contents of the glass (2σ deviations based on replicate IR measurements), in the amounts of water loaded into the capsule via microsyringe (± 11 μmole), and in weighing error (± 0.0001 g) on the amount of glass starting material. Because the molecular weight of $Ag_2C_2O_4$ is large (and therefore weighing error will not significantly affect the amount of CO_2 loaded into a capsule) and little CO_2 is dissolved in the glass at the end of an experiment, mass balance errors for CO_2 are estimated to be very small ($\approx < 1$ μmol).

[b] Precision for the manometric measurements is ± 0.3 μmole.

[c] Based on analyses of 15 glass chips from the same rhyolite starting material. Mean bulk water content was 0.16 ± 0.06 (2σ) wt% total water [38]. Numbers in parentheses are propagated 2σ uncertainties.

[d] Total water determined from the sum of H_2O_{mol} and water dissolved as OH^-, except for Experiment 9, in which the amount of H_2O_{mol} was below detection. For Experiment 9, total water was determined by the peak height of the absorption at 3550 cm^{-1} [34]. Numbers in parentheses indicate 2σ deviations determined from the distribution of IR measurements.

[e] From IR spectroscopic measurement of H_2O_{mol} absorbance at 5200 cm^{-1} and OH^- absorbance at 4500 cm^{-1} [9]. Molecular water in glass from Experiment 9 was determined by subtracting the amount of OH^- determined by the 4500 cm^{-1} band from the amount of total water determined from the 3550 cm^{-1} band.

[f] Equilibrium concentration of molecular water at 850°C calculated using the regular solution model parameters of Zhang et al. [51]. See caption to Fig. 3.

[g] Determined using the peak height of molecular CO_2 absorption at 2350 cm^{-1} [38,39]. Numbers in psrentheses indicate 2σ determined from the distribution of IR measurements.

[h] *m* = microlites; *c* = clear glass; *b* = bubbles present.

expect up to 2% of the gas to be CO plus H_2 (CH_4 would be negligible) in the most CO_2-rich runs (and less in the more H_2O-rich runs) [41]. The measured abundances of non-condensable gases such as CO and H_2 are even lower than these low abundances expected based on f_{H_2} equilibration [41]. Although the reason for this is not clear, the observation of low amounts of non-condensable gases combined with the close agreement between the manometric and calculated CO_2 and H_2O yields indicate that the proportions of other C-O-H gases in our experiments are very small.

3.1 CO_2

Concentrations of CO_2 molecules in the quenched glasses (expressed as mole fraction of dissolved CO_2 in the melt, $X^{m}_{CO_2}$) are plotted in Fig. 2a vs. the fugacity of CO_2 (f_{CO_2}) in the vapor (based on a modified Redlich–Kwong equation of state for the vapor [43]). The fugacity of CO_2 in the mixed H_2O–CO_2 experiments is directly proportional to the mole fraction of dissolved molecular CO_2, demonstrating clearly that Henry's Law is satisfied for molecular CO_2 in rhyolitic melts coexisting with H_2O–CO_2 vapor under these conditions. In particular, there is no suggestion of an increase in the amount of CO_2 dissolved in vapor-saturated melt as $X^{v}_{CO_2}$ decreases from 1. This result is very different from that obtained for albite liquid at 20 kbar and 1450°C, where the dissolved CO_2 content was observed to increase by $\approx 50\%$ as $X^{v}_{CO_2}$ decreased from 1.0 to 0.8 [44]. Mysen [44] observed that the enhancement of CO_2 solubility in aluminosilicate melts by the addition of water at 10–30 kbar and 1450–1625°C diminishes with increasing temperature and with decreasing pressure. Other studies of melts equilibrated with H_2O–CO_2 fluids at 5–40 kbar [29–33] report smaller but still significant enhancements of CO_2 solubility by

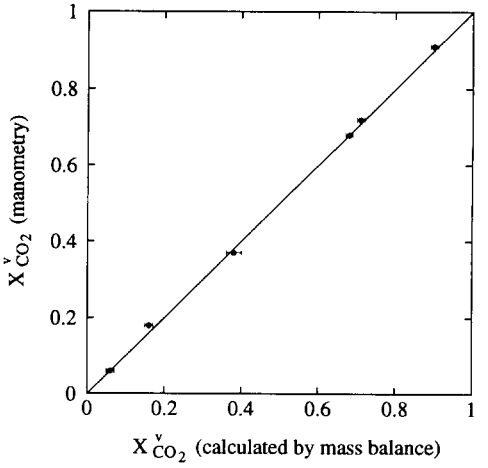

Fig. 1. Comparison of $X^{v}_{CO_2}$ based on manometry and mass balance constraints. Errors on manometric measurements are smaller than the symbols. Errors on $X^{v}_{CO_2}$ calculated from mass balance are based on propagation of errors in concentrations of water and carbon dioxide in the starting and quenched glasses (based on 2σ for the distribution of replicate spectroscopic measurements of dissolved CO_2 or H_2O contents) and weighing errors on the amounts of each starting material (water, silver oxalate, glass) loaded into the capsule.

addition of water for similar or lower values of $X^{v}_{CO_2}$. If these earlier results are correct and applicable to rhyolitic melts, the much smaller *amount* of water dissolved at $X^{v}_{CO_2} = 0.8$ at 750 bar compared to 20 kbar might explain the difference between our result and those obtained at higher pressures. In other words, since only 1–2 wt% water is dissolved in melt coexisting with vapor with $X^{v}_{CO_2} = 0.8$ at 750 bar but ~ 5–10 wt% water is dissolved in melt coexisting with this vapor at 20 kbar, the amount of dissolved water at lower pressures may simply not be sufficient to have a measurable effect on CO_2 dissolution. If this is the correct explanation of the difference between the low and high pressure results, it could imply that solution of water as H_2O molecules rather than as hydroxyl groups plays the major role in stabilizing excess dissolved CO_2

[i] **Mole fraction calculations**: $X^{v}_{CO_2}$ is defined by (μmole CO_2 vapor)/(μmole CO_2 vapor + H_2O vapor); 2σ propagated errors for mass balance estimate of $X^{v}_{CO_2}$ are given in parentheses. $X^{m}_{CO_2}$ calculated by (wt% CO_2/44)/[(100 − wt% H_2O_{tot} − wt% CO_2)/32.5 + (wt% H_2O_{tot}/18) + (wt% CO_2/44)] where 32.5 is the molecular weight of anhydrous rhyolite on a one-oxygen basis. X_B (bulk water) = (wt% H_2O_{tot}/18)/((100 − wt% H_2O_{tot} − wt% CO_2)/32.5 + (wt% H_2O_{tot})/18 + (wt% CO_2)/44] X_{H_2Omol} = (wt% H_2O_{mol}/18)/[(100 − wt% H_2O_{tot})/32.5 + (wt% H_2O_{tot})/18 + (wt% CO_2)/44].

[j] Fugacities calculated using a modified Redlich–Kwong equation of state [43] based on $X^{v}_{CO_2}$ determined from manometric measurements.

since there are already substantial amounts of water dissolved as hydroxyl groups at 1–2 wt% dissolved water, and most additional dissolved water beyond this level is added as H_2O molecules [23].

The Henrian behavior of CO_2 in the melt is clearly indicated in Fig. 2b by the 1:1 correspondence between the activity of CO_2 in the vapor and the ratio of the concentration of CO_2 in the rhyolitic melt saturated with H_2O–CO_2 vapor to its concentration in melt saturated with pure CO_2 vapor at this pressure and temperature. The latter is equivalent to the activity of CO_2 in the melt given a Henry's Law standard state taken as CO_2 in the melt saturated with pure CO_2 vapor at P and T. The activity of CO_2 in the vapor is the ratio of the CO_2 fugacity in a mixed CO_2–H_2O experiment to that of pure CO_2 vapor at the pressure and temperature of the the mixed-volatile experiments, namely 750 bar and 850°C; for a vapor that obeys the Lewis–Randall rule, which H_2O–CO_2 approximately does under these conditions, this is equivalent to $X^{v}_{CO_2}$.

The open symbols in Fig. 2a show the variation in solubility of CO_2 in rhyolitic melt saturated with pure CO_2 vapor at 850°C vs. f_{CO_2} where the variation in f_{CO_2} is achieved by varying total pressure (as opposed to the constant pressure experiments reported here, in which the variation in f_{CO2} is due to dilution of the vapor with H_2O); the dashed curve shows the fit to these data using the formulation given by [45]. The concave-downward curvature of this fit to the open symbols in Fig. 2a, which becomes more pronounced at higher pressures, reflects the finite partial molar volume of CO_2 in rhyolitic melt (28 ± 2 cm^3/

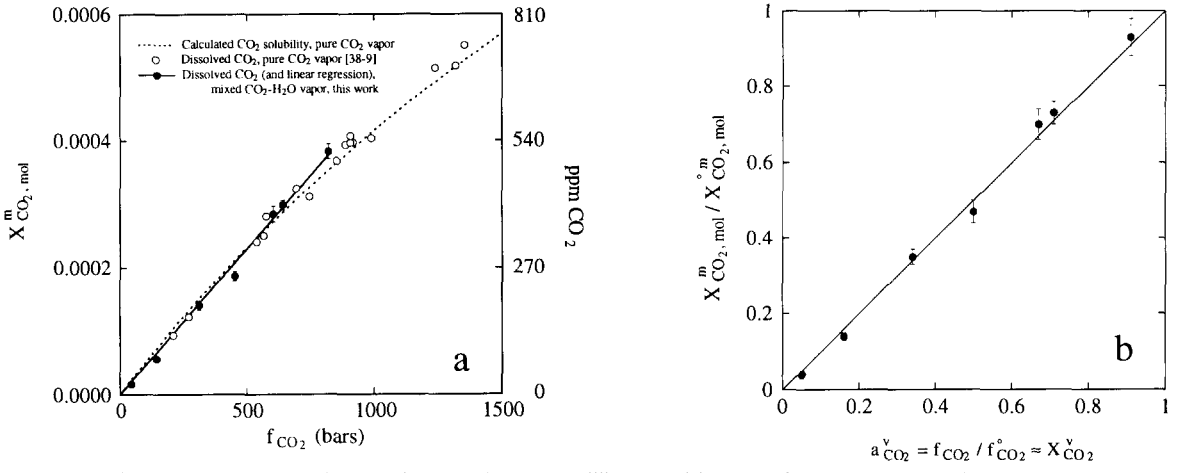

Fig. 2. Henrian behavior of CO_2 dissolved in rhyolitic melt equilibrated with pure CO_2 vapor or a mixed CO_2–H_2O vapor at 850°C and 750 bar, as shown by the following: (a) The proportionality of dissolved molecular CO_2 in vapor-saturated rhyolitic melt to f_{CO_2}. Results for melts in equilibrium with mixed H_2O–CO_2 vapor at constant total pressure (●; this work) are compared with results for melts in equilibrium with essentially pure CO_2 vapor over a range of pressures (○; [38]). Fugacities were calculated using a modified Redlich–Kwong equation of state [43]. Errors on mixed-volatile data are 2σ. The solid line is a regression through the mixed-volatile data forced through the origin: $X^{m}_{CO_2} = (4.6 \pm 0.1) \times 10^{-7}\ f_{CO_2}$, or ppm $CO_2 = (6.2 \pm 0.1) \times 10^{-1}\ f_{CO_2}$ where $r^2 = 0.99$. The dashed curve is the calculated concentration of CO_2 in rhyolitic melt coexisting with pure CO_2 vapor at 850°C, where $P_{CO_2} \approx P_{total}$. This curve was calculated using eq. (4) from Stolper et al. [45] and data of Blank [38] and Fogel and Rutherford [21], from which the following parameters were derived: the partial molar volume of molecular CO_2 in the melt, $v^{m}_{CO_2} = 28(\pm 2)$ cm^3/mole (assumed independent of P and T) the molar enthalpy change for CO_2 dissolution in the melt, $\Delta H°_{CO_2}(P_o) = -27.2(\pm 2.1)$ kJ/mole (assumed independent of T) $\ln[X^{om}_{CO_2}(P_o,T_o)/f^{o}_{CO_2}(P_o,T_o)] = -14.45(\pm 0.02)$, where the reference P and T (P_o, T_o) are 1 bar, 850°C. (b) Comparison between the activity of CO_2 in the H_2O–CO_2 vapor coexisting with the rhyolitic melt (i.e., the ratio of the fugacity of CO_2 in the experiment to the fugacity of pure CO_2 vapor at the pressure and temperature of the experiment) and the ratio of the concentration of CO_2 in the H_2O–CO_2 vapor-saturated rhyolitic melt to its concentration in melt saturated with pure CO_2 vapor at this pressure and temperature (which is equivalent to the activity of CO_2 in the melt given a Henry's Law standard state taken as CO_2 in the melt saturated with pure CO_2 vapor at P and T). The 1:1 line corresponds to Henrian behavior. Data for rhyolite–CO_2 at 750 bar and 850°C used to normalize our mixed-volatile results are: $f^{o}_{CO_2} = 906$ bar, $X^{om}_{CO_2} = 3.97(\pm 0.07) \times 10^{-4}$ [38]. Uncertainties are based on propagation of 2σ errors [55].

mole, [36]). Although this curve is in excellent agreement with the results of our mixed-volatile solubility experiments (the closed symbols in Fig. 2a), the correspondence cannot be exact even if Henry's Law is strictly obeyed. This is because in experiments such as those reported here in which the variation in f_{CO_2} is due to dilution at constant pressure rather than to variable total pressure, a Henrian relationship between solubility and fugacity will be strictly proportional, with no curvature. There is a suggestion of this difference in Fig. 2a, in which the mixed-volatile experiments are better fit by a straight line passing through the origin (solid curve) than by the slightly curved relationship that best fits the pure CO_2 vapor experiments. Although not actually resolvable given the uncertainties in our data, such a difference should become more pronounced as the total pressure increases.

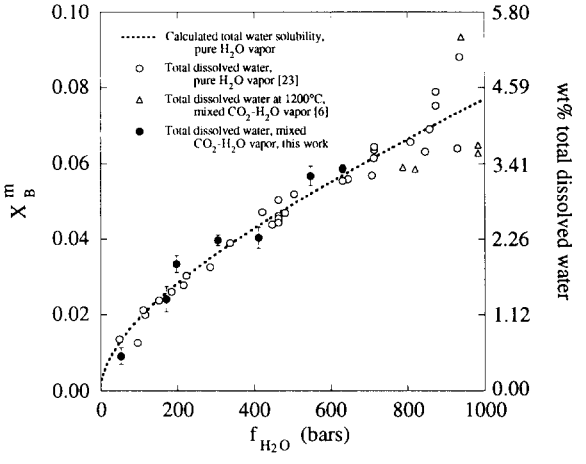

Fig. 3. *Total* dissolved water (water dissolved as OH+ molecular H_2O) content of vapor-saturated rhyolitic melt (expressed as X_B, calculated on a single-oxygen basis [23,47]) vs. f_{H_2O}. Fugacities were calculated using a modified Redlich–Kwong equation of state [43]. 850°C mixed-volatile results from this work (●); 1200°C mixed-volatile results of Kadik et al. [6] (△) and 850°C pure water vapor results of Silver et al. [23] (○). Errors on mixed-volatile data are 2σ. The dashed curve is the best-fit concentration of H_2O in rhyolitic melt coexisting with pure H_2O vapor (where f_{H_2O} varies due to changes in total pressure) and was calculated by the method outlined in Silver et al. [23] (see their fig. 13a) using bulk water data from Silver et al. [23] and Karsten et al. [49], and equilibrium molecular water contents calculated from bulk water data using the regular solution model parameters given by Zhang et al. ([51]; see caption to their fig. 6). Best-fit thermodynamic parameters used in the calculations are: $\upsilon^m_{H_2O} = -2.5(\pm 3.0)$ cm^3/mole $\Delta H^\circ_{H_2O}$ $(P_o) = -26.6$ (± 4.4) kJ/mole $\ln[X^o_{H_2Omol}$ $(P_o, T_o)/f^o_{H_2O}$ $(P_o, T_o)] = -10.31(\pm 0.04)$ where (P_o, T_o) are 1 bar and 850°C.

3.2 H_2O

The interaction between water and rhyolitic melt at these pressures is more complex than for CO_2 in that water molecules dissolve directly in the melt and also react with it to generate hydroxyl groups [46]. Consequently, the relationship between total dissolved water content (expressed as X^m_B), the mole fraction of water calculated on a single oxygen basis [23,47]) and the fugacity of water (f_{H_2O}) is roughly parabolic (Fig. 3). Note in Fig. 3 that the results of our mixed-volatile experiments fall on the same trend as that of experiments in which rhyolitic melts were equilibrated with pure water vapor [23], demonstrating that the activity coefficient for bulk water in rhyolitic melt is insensitive to the low concentrations of dissolved carbon dioxide in these experiments. Also included in Fig. 3a are data from an early study by Kadik et al. [6] on the solubilities of CO_2 and H_2O in rhyolitic melts. These authors measured bulk water and CO_2 dissolved in the glasses using a gravimetric method. Although the measured CO_2 contents of their quenched glasses are an order of magnitude higher than our values, their measured water contents for experiments conducted at 1200°C agree well with ours. This agreement is consistent with the small temperature dependence of water solubility in silicate melts noted by previous workers [e.g., 48–50].

Henrian behavior for dissolved water can be demonstrated by showing that the concentration of dissolved *molecular* water is proportional to f_{H_2O} or $a^v_{H_2O}$, the activity of water in the vapor [23]. This is shown in Figs. 4a and b for our dataset using previously determined relationships between total water content, molecular water content and temperature [23,51]. Note that we have the corrected the observed H_2O_{mol} concentrations to account for changes in dissolved water speciation during quenching of the rhyolitic glasses [35]. The validity of Henry's Law for molecular water in rhyolitic melts containing both dissolved water and carbon dioxide, as has been previously demonstrated for a range of compositions containing dissolved water only [23,47],

demonstrates a negligible influence of CO_2 on the solution behavior of water; this is not surprising given the very low concentrations of CO_2 in the quenched glasses. Note that over the pressure range we have investigated there is no discernible difference between the solubility curve for molecular water dissolved in rhyolitic melt equilibrated with pure water vapor and a best-fit line defined by the mixed-volatile results (Fig. 4a). As discussed for CO_2 solubility above, some deviation between the constant pressure–variable vapor composition results and the pure water vapor–variable total pressure results must exist given the finite partial molar volume of water in rhyolitic melt, but this would only be detectable at pressures much higher than those that we have studied [23].

4. Conclusions

Our results demonstrate that, under the conditions of our experiments, which are relevant to degassing of common silicic magmas near the earth's surface, Henry's Law is obeyed for both molecular water and carbon dioxide in rhyolitic melts. Thus, the amount of CO_2 dissolved in a rhyolitic melt saturated with H_2O–CO_2 vapor at a given pressure and temperature will be lower than if the vapor were pure CO_2 by a factor equal to the ratio of the fugacity of CO_2 in the mixed vapor to the fugacity of CO_2 in pure CO_2 vapor at the same conditions. This is essentially a dilution effect. The same is true for the amount of water dissolved in the melt, except that it is the amount of molecular water that is lowered pro-

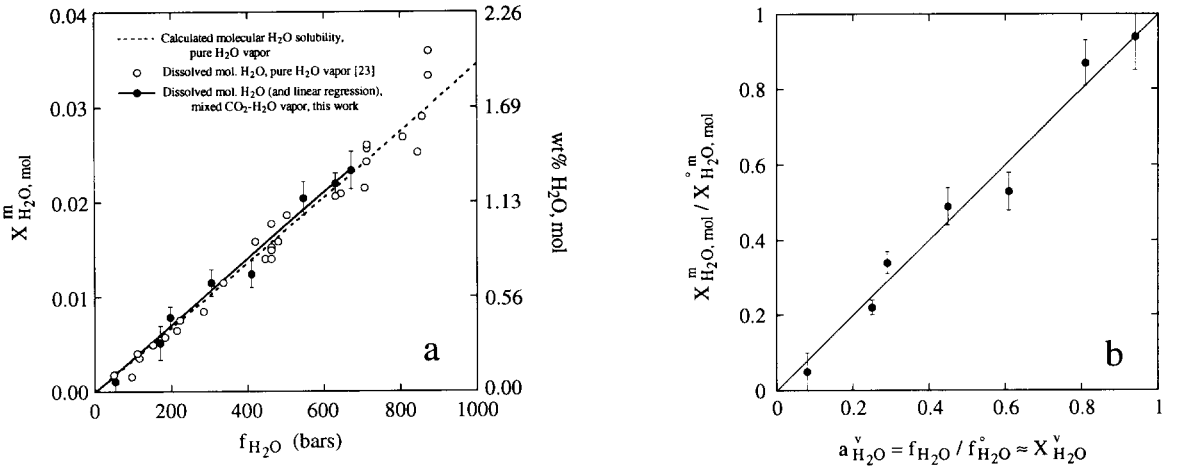

Fig. 4. Illustration of Henrian behavior of molecular water dissolved in rhyolitic melt equilibrated with a pure H_2O vapor or a mixed CO_2–H_2O vapor at 850°C and 750 bar, as shown by the following: (a) The proportionality of dissolved molecular water in vapor-saturated rhyolitic melt to f_{H_2O}. Results for melts in equilibrium with mixed H_2O–CO_2 vapor at constant total pressure (●; this work) are compared with results for melts in equilibrium with essentially pure H_2O vapor over a range of pressures (○; [23]). Fugacities were calculated using a modified Redlich–Kwong equation of state [43]. Errors on mixed-volatile data are 2σ. Concentrations of dissolved molecular water in rhyolitic glasses have been calculated at 850°C based on the regular solution model parameters of Zhang et al. [51]. The solid line is a linear regression through the mixed-volatile data forced through the origin: $X^{m}_{H_2Omol} = (3.5 \pm 0.1) \times 10^{-5}\ f_{H_2O}$, or wt% $H_2O_{mol} = (19.8 \pm 0.6) \times 10^{-4}\ f_{H_2O}$, with $r^2 = 0.98$. The dashed curve is the calculated concentration of molecular H_2O in rhyolitic melt coexisting with pure H_2O vapor at 850°C, where $P_{H_2O} \approx P_{total}$, based on the best-fit parameters given in the caption to Fig. 3. (b) Comparison between the activity of H_2O in the H_2O–CO_2 vapor coexisting with the rhyolitic melt (i.e., the ratio of the fugacity of H_2O in the experiment to the fugacity of pure H_2O vapor at the pressure and temperature of the experiment) and the ratio of the concentration of molecular H_2O in the CO_2–H_2O vapor-saturated rhyolitic melt to its concentration in melt saturated with pure H_2O vapor at this pressure and temperature (which is equivalent to the activity of H_2O in the melt given a Henry's Law standard state taken as molecular H_2O in the melt saturated with pure H_2O vapor at P and T). The 1:1 line corresponds line to Henrian behavior. Data for rhyolite–H_2O at 750 bar and 850°C used to normalize our mixed-volatile results are: $f^{o}_{H_2O} = 672$ bar (for $P_{tot} = P_{H_2O}$) and $X^{om}_{H_2Omol} = 0.0234(\pm 0.0020)$ [38]. Errors are based on propagation of 2σ errors [55].

portionately to the fugacity of water by this dilution effect. There is no evidence of an enhancement of CO_2 solubility in mixed H_2O–CO_2 systems over systems in which only CO_2 is present, contrary to previous reports for significantly higher pressures [7,19,29–31,33]. Henrian behavior has also been reported recently for H_2O–CO_2–basalt [52,53] and for CO_2–CO–basalt [54] at pressures under 1 kbar. While it is not surprising that the small amounts of CO_2 that dissolve in the melt have little influence on the solubility of water and thus that Henry's Law is obeyed for molecular water for the full range of vapor compositions, the situation for CO_2 is different. Water has a significant effect on melt structure and is not a minor component of the melt in our experiments, so it would not be surprising if, as has been observed in other melt compositions at significantly higher total pressures, solution of water influenced the solubility mechanisms and thermodynamics of dissolved CO_2. Further work will be needed to characterize the transition between the observed Henrian behavior at low pressure and reported non-Henrian behavior at elevated pressures and the implied significance for solubility mechanisms under these conditions. However, it appears that efforts to model high-level crustal and volcanic phenomena are considerably simplified by the validity of Henry's Law for the major volatile species.

Acknowledgements

We thank T. Gerlach, M. Rutherford, T. Sisson and T. Trull for their careful reviews. This work was funded by NASA grant NGT-50501, by NSF grants EAR89-16707 and 92-19899, and by DOE grant DE-F603-85ER13445. This is Division of Geological and Planetary Sciences contribution 5157.

References

1 T.A. Jagger, Magmatic gases, Am. J. Sci. 238, 313–353, 1940.
2 W.S. Fyfe, N.J. Price and A.B. Thompson, Fluids in the Earth's Crust, 383 pp., Springer, 1970.
3 A.T. Anderson, Some basaltic and andesitic gases, Rev. Geophys. Space Phys. 13, 37–55, 1975.
4 T.M. Gerlach and B.E. Nordlie, The C-H-O-S gaseous system. Part I: Composition limits and trends in basaltic gases. Part II: Temperature, atomic composition and molecular equilibria in volcanic gases. Part III: Magmatic gases compatible with oxides and sulfides in basaltic magmas, Am. J. Sci. 275, 353–410, 1975.
5 P. Allard, J. Carbonnelle, D. Dajlevic, J. Le Bronec, P. Morel, M.C. Robe, J.M. Maurenas, R. Faivre-Pierret, D. Martin, J.C. Sabroux and P. Zettwoog, Eruptive and diffusive emissions of CO_2 from Mount Etna, Nature 351, 387–391, 1991.
6 A.A. Kadik, O.A. Lukanin, Y.B. Lebedev and E.Y. Kolovushkina, Solubility of H_2O and CO_2 in granite and basalt melts at high pressures, Geochem. Int. 9, 1041–1050, 1972.
7 J.R. Holloway, Volatile interactions in magmas, in: Thermodynamics of Melts and Minerals, R.C. Newton, A. Navrotsky and B.J. Wood, eds., pp. 273–293, Springer, New York, 1981.
8 T.M. Gerlach and D.M. Thomas, Carbon and sulphur isotopic composition of Kilauea parental magma, Nature 319, 480–483, 1986.
9 S. Newman, E.M. Stolper and S. Epstein, Measurement of water in rhyolitic glasses: Calibration of an infrared spectroscopic technique, Am. Mineral. 71, 1527–1541, 1986.
10 A.T. Anderson, Jr., S. Newman, S.N. Williams, T.H. Druitt, C. Skirius and E. Stolper, H_2O, CO_2, Cl and gas in plinian and ash-flow Bishop rhyolite, Geology 17, 221–225, 1989.
11 T.H. Druitt, R.A. Mellors, D.M. Pyle and R.S.J. Sparks, Explosive volcanism on Santorini, Greece, J. Geophys. Res. 93, 15314–15328, 1989.
12 S. Tait and C. Jaupart, Dynamics of eruptive phenomena, Rev. Mineral. 24, 125–152, 1990.
13 H.D. Holland, The Chemical Evolution of the Atmosphere, 582 pp., Princeton University Press, Princeton, 1984.
14 R.W. Goranson, The solubility of water in granite magmas, Am. J. Sci. 22, 481–502, 1931.
15 N.I. Khitarov, E.B. Lebedev, E.V. Rengarten and R.V. Arseneiva, Comparative characteristics of the solubility of water in basaltic and granitic melts, Geokhimiya 5, 479–492, 1959.
16 D.L. Hamilton, C.W. Burnham and E.F. Osborn, The solubility of water and effects of oxygen fugacity and water content on crystallization in mafic magmas, J. Petrol. 5, 21–39, 1964.
17 A.A. Kadik and O.A. Lukanin, The solubility-dependent behavior of water and carbon dioxide in magmatic processes, Geochem. Int. 10, 115–129, 1973.
18 A.A. Kadik and O.A. Lukanin, Paths of mantle outgassing during melting: The role of partial melting of upper mantle rocks in the evolution of fluid composition and redox regime, Int. Geol. Rev. 27, 563–572, 1985.
19 B.O. Mysen, D.H. Eggler, M.G. Seitz and J.R. Holloway, Carbon dioxide solubilities in silicate melts and crystals. Part I. Solubility measurements, Am. J. Sci. 276, 455–479, 1976.
20 E.M. Stolper and J.R. Holloway, Experimental determination of the solubility of carbon dioxide in molten basalt at low pressure, Earth Planet. Sci. Lett. 87, 397–408, 1988.
21 R.A. Fogel and M.J. Rutherford, The solubility of carbon

dioxide: A quantitative FTIR study, Am. Mineral. 75, 1311–1326, 1990.
22 S.N. Shilobreyeva and A.A. Kadik, Solubility of CO_2 in magmatic melts at high temperatures and pressures, Geochem. Int. 27, 31–41, 1990.
23 L.A. Silver, P.D. Ihinger and E. Stolper, The influence of bulk composition on the speciation of water in silicate glasses, Contrib. Mineral. Petrol. 104, 142–162, 1990.
24 T.M. Gerlach and E.J. Graeber, Volatile budget of Kilauea Volcano, Nature 313, 273–277, 1985.
25 S. Newman, S. Epstein and E. Stolper, Water, carbon dioxide, and hydrogen isotopes in glasses from the ca. 1340 A.D. eruption of the Mono Craters, California: Constraints on degassing phenomena and initial volatile content, J. Volcanol. Geotherm. Res. 35, 75–96, 1988.
26 H.R. Westrich, H.W. Stockman and J.C. Eichelberger, Degassing of rhyolitic magma during ascent and emplacement, J. Geophys. Res. 93, 6503–6511, 1988.
27 C.M. Skirius, Pre-eruptive H_2O and CO_2 content of plinian and ash-flow Bishop Tuff magma, Ph.D. Dissert., Univ. Chicago, 1990.
28 T.A. Vogel, J.C. Eichelberger, L.W. Younker, B.C. Schuraytz and J.P. Horkowitz, Petrology and emplacement dynamics of intrusive and extrusive rhyolites of Obsidian Dome, Inyo Craters volcanic chain, eastern California, J. Geophys. Res. 17, 17937–17956, 1991.
29 J.R. Holloway and C.F. Lewis, CO_2 solubility in hydrous albite liquid at 5 kbar, EOS 55, 483, 1974.
30 G. Brey and D.H. Green, The role of CO_2 in the genesis of olivine melilitite, Contrib. Mineral. Petrol. 49, 93–103, 1975.
31 G. Brey, CO_2 solubility and solubility mechanisms in silicate melts at high pressures, Contrib. Mineral. Petrol. 57, 215–221, 1976.
32 B.O. Mysen, R.J. Arculus and D.H. Eggler, Solubility of carbon dioxide in melts of andesite, tholeiite, and olivine nephelinite composition to 30 kbar, Contrib. Mineral. Petrol. 53, 227–239, 1975.
33 D. Eggler and M. Rosenhauer, Carbon dioxide in silicate melts: II. Solubilities of CO_2 and H_2O in $CaMgSi_2O_6$ (diopside) liquids and vapors at pressures to 40 kb, Am. J. Sci. 278, 64–94, 1978.
34 P.F. Dobson, S. Epstein and E.M. Stolper, Hydrogen isotope fractionation between coexisting vapor and silicate glasses and melts at low pressure, Geochim. Cosmochim. Acta 53, 2723–2730, 1989.
35 P.D. Ihinger, An experimental study of the interaction of water with granitic melt, Ph.D. Dissert., California Inst. Technol., 1991.
36 J. Bigeleisen, M.L. Perlman and H.C. Prosser, Conversion of hydrogenic materials to hydrogen for isotopic analysis, Anal. Chem. 24, 1356–1357, 1952.
37 J.G. Blank, E.M. Stolper, J. Sheng and S. Epstein, The solubility of CO_2 in rhyolitic melt at pressures less than 1500 bars, Geol. Soc. Am. Abstr. Prog. 21, A157, 1989.
38 J.G. Blank, An experimental investigation of the behavior of carbon dioxide in rhyolitic melt, Ph.D. Dissert., California Inst. Technol., 1993.
39 J.G. Blank and E.M. Stolper, The solublity of CO_2 in rhyolitic melt at pressures up to 1500 bars, in prep.
40 G. Fine, Carbon dioxide in synthetic and natural silicate glasses, Ph.D. Dissert., California Inst. Technol., 1986.
41 J.R. Holloway and R.L. Reese, The generation of N_2-CO_2-H_2O fluids for use in hydrothermal experimentation I. Experimental method and equilibrium calculations in the C-O-H-N system, Am. Mineral. 59, 587–597, 1974.
42 C.-H. Geschwind and M.J. Rutherford, Cummingtonite and the evolution of the Mount St. Helens (Washington) magma system: An experimental study, Geology 20, 1011–1014, 1992.
43 J.R. Holloway, Fugacity and activity of molecular species in supercritical fluids, in: Thermodynamics in Geology, D. Fraser, ed., pp. 161–181, Reidel, Boston, 1977.
44 B.O. Mysen, The role of volatiles in silicate melts: Solubility of carbon dioxide and water in feldspar, pyroxene, and feldspathoid melts to 30 kb and 1625°C, Am. J. Sci. 276, 969–996, 1976.
45 E. Stolper, G. Fine, T. Johnson and S. Newman, Solubility of carbon dioxide in albitic melt, Am. Mineral. 72, 1071–1085, 1987.
46 E. Stolper, Water in silicate glasses: An infrared spectroscopic study, Contrib. Mineral. Petrol. 81, 1–17, 1982.
47 L.A. Silver and E. Stolper, Water in albitic glasses, J. Petrol. 30, 667–709, 1989.
48 C.W. Burnham and R.H. Jahns, A method for determining the solubility of water in silicate melts, Am. J. Sci. 260, 721–745, 1962.
49 J.L. Karsten, J.R. Holloway and J.R. Delaney, Ion microprobe studies of water in silicate melts: Temperature-dependent water diffusion in obsidian, Earth Planet. Sci. Lett. 59, 420–428, 1982.
50 E.M. Stolper, Temperature dependence of the speciation of water in rhyolitic melts and glasses, Am. Mineral. 74, 1247–1257, 1989.
51 Y. Zhang, E.M. Stolper and G.J. Wasserburg, Diffusion of water in rhyolitic glasses, Geochim. Cosmochim. Acta 55, 441–456, 1991.
52 J.E. Dixon, E.M. Stolper and J.R. Holloway, Solubilities of water and carbon dioxide in basaltic magmas, Geol. Soc. Am. Abstr. Prog. A93, 1991.
53 J.E. Dixon, Water and carbon dioxide in basaltic magmas, Ph.D. Dissert., California Inst. Technol., 1992.
54 A.R. Pawley, J.R. Holloway and P. McMillan, The effect of oxygen fugacity on the solubility of carbon–oxygen fluids in basaltic melt, Earth Planet. Sci. Lett. 110, 213–225, 1992.
55 P.R. Bevington, Data Reduction and Error Analysis for the Earth Sciences, 336 pp., McGraw-Hill, San Francisco, 1969.